Bioorganic & Medicinal Chemistry Letters xxx (xxxx) xxxx

Contents lists available at ScienceDirect

Bioorganic & Medicinal Chemistry Letters

journal homepage: www.elsevier.com/locate/bmcl

A new chemotype with promise against *Trypanosoma cruzi*

Xiaofang Wang[a], Monica Cal[b,c], Marcel Kaiser[b,c], Frederick S. Buckner[d], Galina I. Lepesheva[e], Austin G. Sanford[f], Alexander I. Wallick[f], Paul H. Davis[f], Jonathan L. Vennerstrom[a,*]

[a] College of Pharmacy, University of Nebraska Medical Center, 986025 Nebraska Medical Center, Omaha, NE, United States
[b] Department of Medical Parasitology and Infection Biology, Swiss Tropical Institute, Socinstrasse 57, CH-4002 Basel, Switzerland
[c] University of Basel, CH-4003 Basel, Switzerland
[d] Department of Medicine, University of Washington, 750 Republican Street, Seattle, WA, United States
[e] Department of Biochemistry, Vanderbilt University, 2200 Pierce Ave., Nashville, TN, United States
[f] Department of Biology, University of Nebraska at Omaha, Omaha, NE, United States

ARTICLE INFO

Keywords:
Chagas disease
Trypanosoma cruzi
SAR

ABSTRACT

Pyridyl benzamide **2** is a potent inhibitor of *Trypanosoma cruzi*, but not other protozoan parasites, and had a selectivity-index of ≥10. The initial structure–activity relationship (SAR) indicates that benzamide and sulfonamide functional groups, and *N*-methylpiperazine and sterically unhindered 3-pyridyl substructures are required for high activity against *T. cruzi*. Compound **2** and its active analogs had low to moderate metabolic stabilities in human and mouse liver microsomes.

Chagas disease, endemic in over 20 Latin American countries, is a vector-borne infection with the protozoan parasite *Trypanosoma cruzi*.[1,2] The nitroaromatic drugs nifurtimox and benznidazole are effective against the acute phase of the disease, but are less useful against the chronic stage.[1] Both of these drugs have relatively low therapeutic indices and are poorly tolerated. Fexinidazole, another nitroaromatic compound, and two azole antifungal drugs, posaconazole and fosravuconazole, are in clinical trials for Chagas disease.[3] However, for the latter two drugs, there was recrudescence after treatment ceased, indicating a lack of trypanocidal activity. Thus, we need better drugs for this neglected parasitic disease.

We were interested in identifying new hit compounds against pathogenic protozoa by starting with known glucose transporter (GLUT) inhibitors[4] and modifying structure to enable selective inhibition of protozoal hexose transporters[5] and parasite growth. We chose to start with pyridyl benzamide **2**,[6] an optimized analog of the reported GLUT1 inhibitor STF-31 (**1**)[7] Fig. 1). Our initial screen of **2** revealed that it was a potent inhibitor of *T. cruzi*, but not other protozoan parasites. We now describe physicochemical profiling, in vitro ADME, and antiprotozoal activity for **2** and analogs **3–19** designed to establish a baseline structure–activity relationship (SAR) for this chemotype.

Target compounds **2–19** were prepared (Supporting Information) by a variety of reactions described in Schemes 1–4. Compounds **3–9** were prepared in nucleophilic aromatic substitution reactions between aryl fluoride **20**[6] and the requisite secondary amines in moderate (42–64%) yields (Scheme 1). For **3**, a subsequent Boc deprotection with MsOH was required.

Compounds **10–16** were in a two-step sequence starting with carboxylic acid **21**[6] (Scheme 2). The first step was in situ formation of the acid chloride or HOBt active ester of **21** followed by amide bond formation to afford intermediates **22–28**. This was followed by nucleophilic aromatic substitution reactions with 1-methylpiperazine to afford **10–16** in moderate to good (33–72%) yields.

Compounds **17** and **18** were obtained in a two-step reaction sequence (Scheme 3). Reactions of the HOBt active esters of **29**[8] and **30**[9] with 3-aminopyridine afforded **31** (96%) and **32** (97%), respectively. Nucleophilic aromatic substitution reactions of **31** and **32** with 1-methylpiperazine afforded **17** and **18** in moderate yields.

Compound **19** was prepared in moderate yield by converting **21** to **33** by nucleophilic aromatic substitution reaction with 1-methylpiperazine followed by 1,2,4-oxadiazole formation by condensation with *N*-hydroxynicotinimidamide (Scheme 4). Target compounds **2**, **5**, and **6** were prepared following procedures described by Sutphin et al.[6]

In vitro assays with the Tulahuen C4 strain of *Trypanosoma cruzi* were performed as previously described.[10] Data for **2–9** in Table 1 reveal the SAR of the *N*-methylpiperazine substructure of **2**. First, we note that **2** has potent activity against *T. cruzi* with an IC_{50} of 0.007 μM; this compares with an IC_{50} value of 1.2 to 4.2 μM for the benznidazole control. Second, relatively minor structural changes to the *N*-methylpiperazine substructure decreased activity against *T. cruzi* significantly.

* Corresponding author.
E-mail address: jvenners@unmc.edu (J.L. Vennerstrom).

https://doi.org/10.1016/j.bmcl.2019.126778
Received 23 September 2019; Received in revised form 23 October 2019; Accepted 24 October 2019

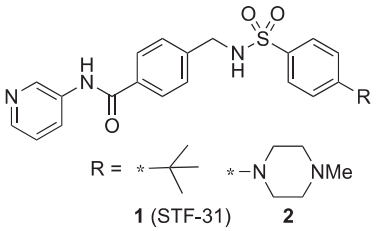

Fig. 1. Structures of STF-31 (**1**) and its analog **2**.

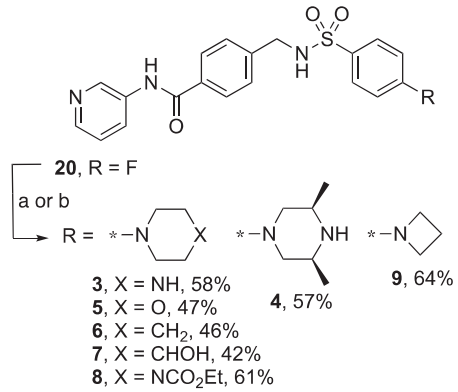

Scheme 1. Reagents and conditions: (a) K_2CO_3, DMA, 110 °C, 20 h and 2,6-*cis*-dimethylpiperazine (**4**), morpholine (**5**), piperidine (**6**), 4-hydroxypiperidine (**7**), ethyl piperazine-1-carboxylate (**8**), or azetidine hydrochloride (**9**); (b) *tert*-butyl piperazine-1-carboxylate (**3**), K_2CO_3, DMA, 110 °C, 20 h, then MsOH, rt, 24 h followed by aq. $NaHCO_3$.

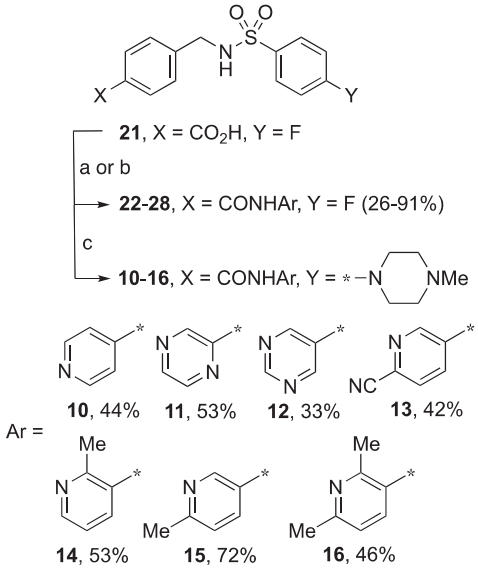

Scheme 2. Reagents and conditions: (a) $SOCl_2$, CH_2Cl_2, 0 °C to 50 °C, 3 h, then 4-aminopyridine (**22**), 2-aminopyrazine (**23**), 5-aminopyrimidine (**24**), or 5-amino-2-pyridinecarbonitrile (**25**); (b) HOBt, EDCl, TEA, DMA, rt, 24 h and 3-amino-2-methylpyridine (**26**), 3-amino-6-methylpyridine (**27**), or 3-amino-2,6-dimethylpyridine (**28**); (c) 1-methylpiperazine, K_2CO_3, DMA, 110 °C, 20 h.

For example, *N*-desmethylpiperazines **3** and **4**, piperidine **6**, piperidinol **7**, and piperazine carbamate **8** were three-orders of magnitude less potent than **2**. Although morpholine **5** and azetidine **9** were also less potent than **2**, they had *T. cruzi* IC_{50} values of 2.1 and 8.3 μM, respectively. For **2–9**, we could discern no clear SAR trends except that a *N*-

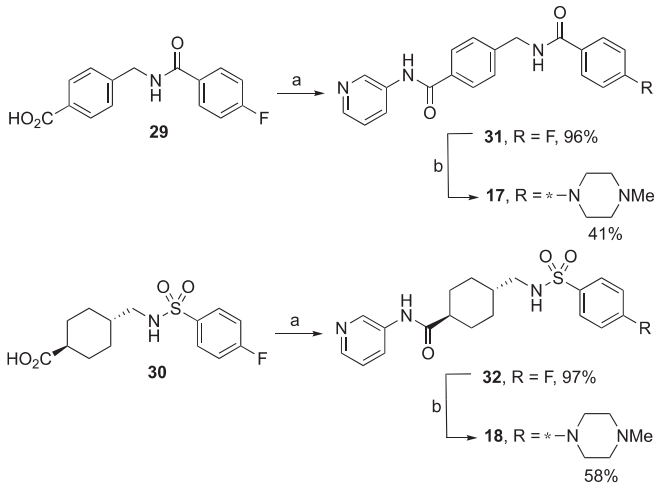

Scheme 3. Reagents and conditions: (a) 3-aminopyridine, HOBt, EDCl, TEA, DMA, rt, 24 h; (b) 1-methylpiperazine, K_2CO_3, DMA, 110 °C, 20 h.

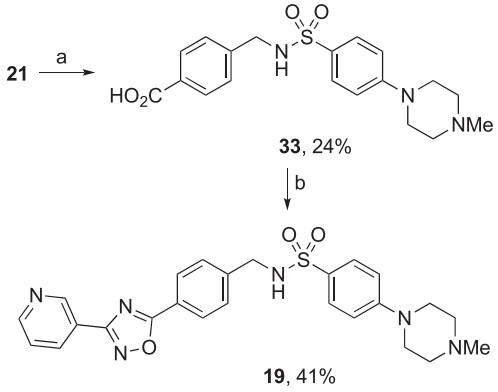

Scheme 4. Reagents and conditions: (a) 1-methylpiperazine, K_2CO_3, DMA, 110 °C, 20 h; (b) *N*-hydroxynicotinimidamide, EDCl, DMA, MW 150 °C, 10 min.

methylpiperazine was the optimal substructure for *T. cruzi* potency.

Data for **10–16** (Table 1) reveals that any change to the 3-pyridyl substructure of **2** reduces potency by three-orders of magnitude. These include other heterocycles (pyrazine **11**, pyrimidine **12**) or substitution with cyano (**13**) or methyl (**14–16**) groups. Finally, the weak activities of **17** and **18** (Table 1) indicate that the sulfonamide and benzamide substructures of **2** are required for high activity against *T. cruzi*. Although **19**, with its 1,2,4-oxadiazole carboxamide isostere, was less potent than **2**, it had a *T. cruzi* IC_{50} value of 1.2 μM.

To assess host cell cytotoxicity, the three most potent compounds **2**, **5**, and **19** were tested for growth inhibition of four human cell lines:[11] foreskin fibroblast (HFF), osteosarcoma (U-2 OS), kidney (HEK 293 T), and hepatocyte (HC-04) (Table 2). Only **5** inhibited the HFF cell line, whereas both **2** and **5** inhibited the U-2 OS and HEK 293 T cell lines with IC_{50} values < 1 μM; the HC-04 cell line was unaffected by all three compounds at concentrations up to 50 μM. Compound **19** was the least cytotoxic of the three. These values compare with previously reported[12] IC_{50} values for **2** ranging from 0.01 to 1 μM against a panel of cancer cell lines.

Compound **2**, **5**, and **19** were tested against a panel of protozoan parasites (Table 3) using the methods of Orhan et al.[10] and Sanford et al.[11] Compound **2** was three-orders of magnitude less potent against *Plasmodium falciparum* and *Trypanosoma brucei rhodesiense* than it was against *T. cruzi* (Table 1) and it had no effect on the growth of

Table 2
Cytotoxicity screen of **2**, **5**, and **19**.

Compd	Cytotoxicity IC_{50} (μM)			
	HFF	U-2 OS	HEK 293 T	HC-04
2	> 50	0.15	0.36	> 50
5	2.0	0.16	0.95	> 50
19	> 50	28	42	> 50

Table 3
Activity of **2**, **5**, and **19** against a panel of protozoan parasites.

Compound	IC_{50} (μM)[a]			
	P. falciparum NF54	*T. b. rhodesiense* STIB 900	*L. donovani*[b] MHOM-ET 67/L82	*T. gondii*[c] RH-dTom
2	10	32	> 200	> 100
5	21	25	180	> 100
19	5.8	3.4	49	21
Drug Standards[d]	0.0042	0.0070	0.99	0.80

[a] Mean from n ≥ 2, individual measurements differed by less than 50%.
[b] The compounds were tested against *L. donovani* amastigotes in an axenic assay.
[c] RH (Type I) strain *T. gondii* with inserted fluorescent transgene dimerized Tomato (dTom).
[d] Chloroquine for *P. falciparum*; melarsoprol for *T. b. rhodesiense*; miltefosine for *L. donovani*; pyrimethamine for *T. gondii.*

Table 4
Physicochemical properties and in vitro metabolic stability of **2**, **5**, and **19**.

Compd	$gLogD_{7.4}$[a]	PSA (Å^2)[b]	$Sol_{2.0}/Sol_{6.5}$ (μg/mL)[c]	h/m CL_{int} (μL/min/mg protein)[d]	cPPB (%)[e]
2	2.8	95.8	> 100/25–50	45/112	85.2
5	2.6	100.6	50–100/12.5–25	69/200	76.2
19	4.1	105.7	> 100/25–50	535/677	not assessed

[a] LogD values were estimated by correlation of their chromatographic retention properties using a modified gradient HPLC method adapted from Lombardo et al.[13]
[b] Calculated using ChemAxon JChem for Excel.
[c] Compounds in DMSO were spiked into either pH 6.5 phosphate buffer or 0.01 M HCl (approx. pH 2.0) and analyzed by nephelometry[14] to determine a concentration range.
[d] In vitro intrinsic clearance measured in human and mouse liver microsomes.
[e] Plasma protein binding was estimated using a gradient HPLC method[15] where the chromatographic retention on a human albumin column was compared against the properties of standard compounds with known binding values.

Leishmania donovani and *Toxoplasma gondii*. Compound **5** was 10-fold less active against *P. falciparum* and *T. b. rhodesiense* than it was against *T. cruzi* (Tables 1 and 3) and it had weak to no activity against the other two protozoans. In contrast, there was little difference in the potency of **19** against *T. cruzi* (Tables 1 and 3), *P. falciparum* and *T. b. rhodesiense*, and it was an order of magnitude less potent against the other two protozoans.

Physicochemical and in vitro ADME properties of **2** and its most potent analogs **5** and **19** are shown in Table 4. The $gLogD_{7.4}$ values ranging from 2.6 to 4.1, calculated polar surface area (PSA) values[16] ranging from 95 and 106 Å^2, aq. solubilities ranging from 12.5 to > 100 μg/mL, and plasma protein binding < 90% suggest that these compounds would be expected to have relatively good biopharmaceutical properties. However, all of the compounds had relatively high intrinsic clearance values in human and mouse liver microsomes indicating that each would be expected to be rapidly metabolized. Metabolic stabilities were higher in human vs. mouse liver microsomes. Compound **19**, the most lipophilic of the three, had the lowest metabolic stability.

In this SAR scoping study, we started with **2**, a known[7] GLUT1 inhibitor. As we did not assess inhibition of glucose transport in *T. cruzi*[17] by **2–19**, we cannot confirm that the *T. cruzi* hexose transporter is a potential cellular target for these compounds. In this respect, a recent study[12] claimed that nicotinamide phosphoribosyltransferase (NAMPT), not GLUT-1, is the target of **1** and **2** in cancer cell lines. In addition, posaconazole and a high proportion of hits identified in HTS campaigns against *T. cruzi* appear to inhibit sterol 14α-demethylase (*T. cruzi* CYP51), and most of these hits contain imidazole or pyridyl substructures.[1,18–21] Of the pyridyl-containing *T. cruzi* CYP51 inhibitors, a sterically unhindered 3-pyridyl substructure was predominant. Thus, we wondered whether *T. cruzi* CYP51 might be a potential target of this compound series based on our observed SAR – particularly the dramatic (three orders of magnitude) loss of potency for **14–16** when methyl groups were introduced adjacent to the nitrogen atom in the 3-pyridyl substructure of **2**.

To test this hypothesis, **2** and **14** were analyzed as *T. cruzi* CYP51 heme binding ligands[22] and for inhibition of enzyme activity in a reconstituted *T. cruzi* CYP51 activity assay.[23] While **2** induced a moderate type II spectral response in the Soret band (K_d 1.32 μM, Fig. 2a), **14** did not cause any changes (not shown). The IC_{50} values, determined in a 30 min reconstituted enzyme reaction, were 49 and 487 μM, respectively (Fig. 2b). These data suggest that CYP51 could be a target for **2** (presumably mediated by binding of pyridine moiety to the heme cofactor of CYP51),[22] although the inhibition at the enzyme level (IC_{50} of 49 μM) does not seem sufficient to fully account for the potency at the cellular level (IC_{50} of 7 nM). For comparison, posoconazole similarly inhibits the growth of *T. cruzi* (IC_{50} of 5 nM), but has a *T. cruzi* CYP51 K_d of 18 nM.[22,24] Thus, the mechanism of action of **2** probably includes another target(s) which is also suggested by the dramatic loss of potency against *T. cruzi* observed with small variations in the *N*-methylpiperazine substructure – e.g. piperazine **3** and morpholine **5**. Finally, the potent activity of **2** on *T. cruzi* and the weak activity against the other protozoa suggest that the target may be highly *T. cruzi* specific.

Declaration of Competing Interest

The authors declare that they have no known competing financial interests or personal relationships that could have appeared to influence the work reported in this paper.

Acknowledgment

We acknowledge the U.S. National Institutes of Health (AI116723-01, GM103427, and GM067871) for financial support. We acknowledge the contributions of the Centre for Drug Candidate Optimisation, Monash University for conducting the ADME studies.

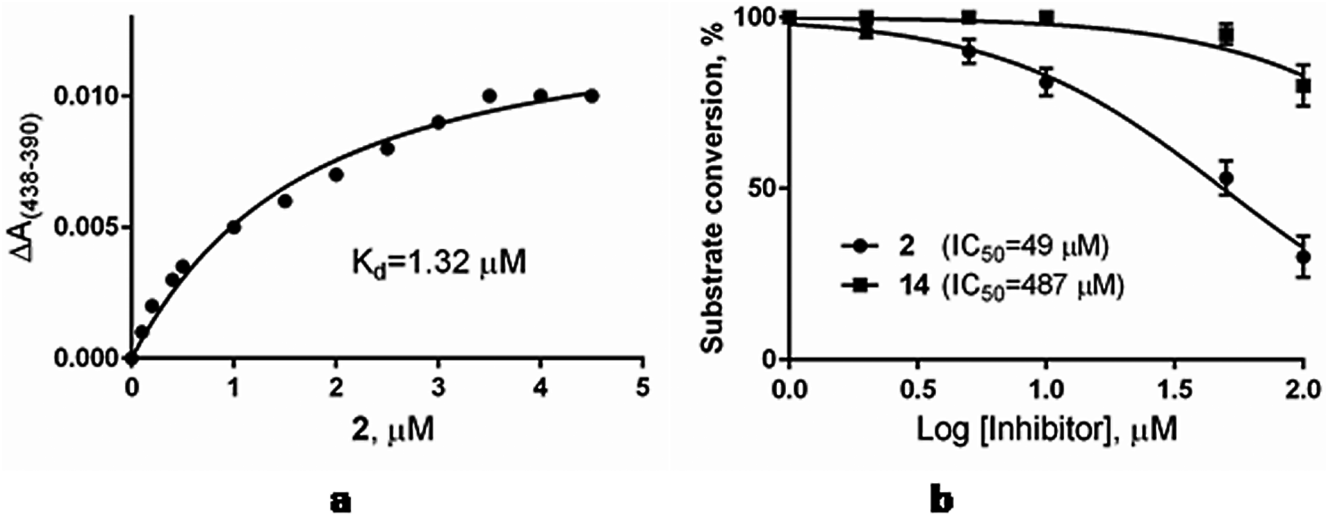

Fig. 2. Ligand binding (a) and inhibition (b) of *T. cruzi* CYP51.

Table 1
In vitro antitrypanosomal activity of **2–19** against the Tulahuen C4 strain of *T. cruzi*.

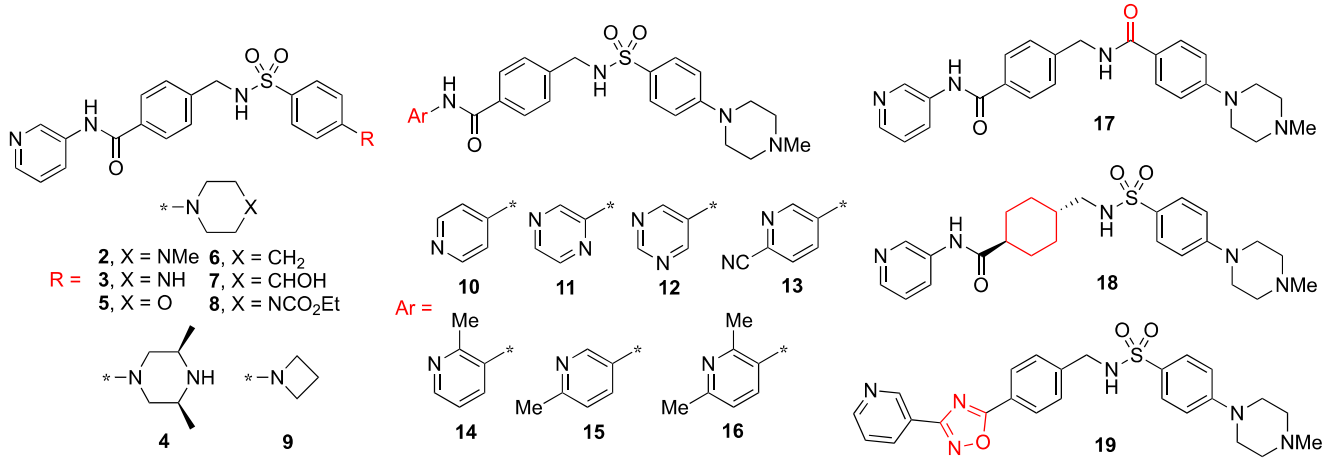

Compd	*T. cruzi* IC_{50} (μM)[a]	Compd	*T. cruzi* IC_{50} (μM)[a]
2	0.007	**11**	17
3	69	**12**	96
4	130	**13**	100
5	2.1	**14**	65
6	110	**15**	88
7	120	**16**	110
8	46	**17**	120
9	8.3	**18**	120
10	28	**19**	1.2

[a] Mean from n ≥ 2, individual measurements differed by less than 50%.

Appendix A. Supplementary data

Supplementary data to this article can be found online at https://doi.org/10.1016/j.bmcl.2019.126778.

References

1. Moraes CB, Franco CH. Novel drug discovery for Chagas disease. *Expert Opin Drug Discov.* 2016;11:447–455.
2. Bermudez J, Davies C, Simonazzi A, Real JP, Palma S. Current drug therapy and pharmaceutical challenges for Chagas disease. *Acta Trop.* 2016;156:1–16.
3. Field MC, Horn D, Fairlamb AH, et al. Anti-trypanosomatid drug discovery: An ongoing challenge and a continuing need. *Nat Rev Microbiol.* 2017;15:217–231.
4. Granchi C, Fortunato S, Minutolo F. Anticancer agents interacting with membrane glucose transporters. *Med Chem Commun.* 2016;7:1716–1729.
5. Ortiz D, Guiguemde WA, Johnson A, et al. Identification of selective inhibitors of the *Plasmodium falciparum* hexose transporter PfHT by screening focused libraries of antimalarial compounds. *PLoS ONE.* 2015;10:e0123598.
6. Sutphin P, Chan D, Turcotte S, et al. Heteroaryl benzamides, compositions and methods of use. 27 January 2011, PCT WO2011011514A1.
7. Chan DA, Sutphin PD, Nguyen P, et al. Targeting GLUT1 and the Warburg effect in renal cell carcinoma by chemical synthetic lethality. *Sci Transl Med.* 2011;3:94ra70.
8. Gálvez AO, Schaack CP, Noda H, Bode JW. Chemoselective acylation of primary amines and amides with potassium acyltrifluoroborates under acidic conditions. *J Am Chem Soc.* 2017;139:1826–1829.

9. Juanenea L, Galiano S, Erviti O, et al. Synthesis and evaluation of new hydrazide derivatives as neuropeptide Y Y5 receptor antagonists for the treatment of obesity. *Bioorg Med Chem.* 2004;12:4717–4723.
10. Orhan I, Sener B, Kaiser M, Brun R, Tasdemir D. Inhibitory activity of marine sponge-derived natural products against parasitic protozoa. *Mar Drugs.* 2010;8:47–58.
11. Sanford AG, Schulze TT, Potluri LP, et al. Novel *Toxoplasma gondii* inhibitor chemotypes. *Parasitol Int.* 2018;67:107–111.
12. Adams DJ, Ito D, Rees MG, et al. NAMPT is the cellular target of STF-31-like small-molecule probes. *ACS Chem Biol.* 2014;9:2247–2254.
13. Lombardo F, Shalaeva MY, Tupper KA, Gao F. $ElogD_{oct}$: a tool for lipophilicity determination in drug discovery. 2. basic and neutral compounds. *J Med Chem.* 2001;44:2490–2497.
14. Bevan CD, Lloyd RS. A high-throughput screening method for the determination of aqueous drug solubility using laser nephelometry in microtiter plates. *Anal Chem.* 2000;72:1781–1787.
15. Valko K, Nunhuck S, Bevan C, Abraham MH, Reynolds DP. Fast gradient HPLC method to determine compounds binding to human serum albumin. Relationships with octanol/water and immobilized artificial membrane lipophilicity. *J Pharm Sci.* 2003;92:2236–2248.
16. Palm K, Stenberg P, Luthman K, Artursson P. Polar molecular surface properties predict the intestinal absorption of drugs in humans. *Pharm Res.* 1997;14:568–571.
17. Tetaud E, Chabas S, Giroud C, Barrett MP, Baltz T. Hexose uptake in *Trypanosoma cruzi*: structure-activity relationship between substrate and transporter. *Biochem J.* 1996;317:353–359.
18. Gunatilleke SS, Calvet CM, Johnston JB, et al. Diverse inhibitor chemotypes targeting *Trypanosoma cruzi* CYP51. *PLoS Negl Trop Dis.* 2012;6:e1736.
19. Keenan M, Chaplin JH, Alexander PW, et al. Two analogues of fenarimol show curative activity in an experimental model of Chagas disease. *J Med Chem.* 2013;56:10158–10170.
20. Keenan M, Alexander PW, Chaplin JH, et al. Selection and optimization of hits from a high-throughput phenotypic screen against *Trypanosoma cruzi*. *Future Med Chem.* 2013;5:1733–1752.
21. Buckner FS, Urbina JA. Recent developments in sterol 14-demethylase inhibitors for Chagas disease. *Int J Parasitol Drugs Drug Resist.* 2012;2:236–242.
22. Hargrove TY, Wawrzak Z, Alexander PW, et al. Complexes of *Trypanosoma cruzi* sterol 14alpha-demethylase (CYP51) with two pyridine-based drug candidates for Chagas disease: structural basis for pathogen selectivity. *J Biol Chem.* 2013;288:31602–31615.
23. Lepesheva GI, Zaitseva NG, Nes WD, et al. CYP51 from *Trypanosoma cruzi*: A phyla-specific residue in the B' helix defines substrate preferences of sterol 14alpha-demethylase. *J Biol Chem.* 2006;281:3577–3585.
24. Villalta F, Dobish MC, Nde PN, et al. VNI cures acute and chronic experimental Chagas disease. *J Infect Dis.* 2013;208:504–511.